AVS Quantum Science ARTICLE scitation.org/journal/aqs

Quantum routing of information using chiral quantum walks

Cite as: AVS Quantum Sci. **5**, 025001 (2023); doi: 10.1116/5.0146805
Submitted: 16 February 2023 · Accepted: 13 April 2023 ·
Published Online: 27 April 2023

Alberto Bottarelli,[1,2,a] Massimo Frigerio,[3,4,b] and Matteo G. A. Paris[3,4,c]

AFFILIATIONS

[1]Pitaevskii BEC Center, CNR-INO and Dipartimento di Fisica, Università di Trento, I-38123 Trento, Italy
[2]INFN-TIFPA, Trento Institute for Fundamental Physics and Applications, Trento, Italy
[3]Quantum Technology Lab & Quantum Mechanics Group, Department of Physics "A. Pontremoli," Università degli Studi di Milano, I-20133 Milano, Italy
[4]Istituto Nazionale di Fisica Nucleare, Sezione di Milano, I-20133 Milano, Italy

Note: This paper is part of the Jonathan P. Dowling Memorial Special Issue.
[a)]**Electronic mail:** alberto.bottarelli@unitn.it
[b)]**Electronic mail:** massimo.frigerio@unimi.it
[c)]**Electronic mail:** matteo.paris@fisica.unimi.it

ABSTRACT

We address routing of classical and quantum information over quantum network and show how to exploit chirality (directionality) to achieve nearly optimal and robust transport. In particular, we prove how continuous-time chiral quantum walks over a minimal graph are able to model directional transfer of information over a network. At first, we show how classical information, encoded onto an excitation localized at one vertex of a simple graph, may be sent to any other chosen location with nearly unit fidelity by tuning a single phase. Then, we prove that high-fidelity transport is also possible for coherent superpositions of states, i.e., for routing of quantum information. Furthermore, we show that by tuning the phase parameter, one obtains universal quantum routing, i.e., independent on the input state. In our scheme, chirality is governed by a single phase, and the routing probability is robust against fluctuations of this parameter. Finally, we address characterization of quantum routers and show how to exploit the self-energies of the graph to achieve high precision in estimating the phase parameter.

I. INTRODUCTION

With the advent of near-future quantum technologies, the problem of transport and routing of energy and quantum information on a network is quickly becoming crucial. In particular, whenever systems with quantum properties are employed to store information locally, its transfer between separate places and its routing toward different target locations is a nontrivial problem. A common strategy is to couple the systems to a field (typically photons) and to use the field as a mediator.[1] However, these protocols may have substantial drawbacks with respect to noise sensitivity and fidelity of the transferred quantum state. Moreover, whenever a large number of transfers are required, the impossibility of amplifying the quantum signal due to the no-cloning theorem makes these issues even more detrimental.

As a matter of fact, quantum spin chains provide a viable alternative for the transport of quantum information on a finite 1D lattice.[2–4] Since this aspect is fully captured in the single excitation subspace of these systems, a fully equivalent description can be provided in the framework of continuous-time quantum walks (CTQW) on graphs.[5–7] However, conventional quantum walks do not allow for directional transport of the excitation because their Hamiltonian generators are real matrices. In order to overcome these limits, one may employ generalized quantum walks whose defining Hamiltonians are hermitian but not required to have only real entries. These are usually termed *chiral* quantum walks, where the chirality refers to the fact that their evolution can break the mirror symmetries of the underlying graph. In this context, they stand out as the simplest generalization to introduce routing in a quantum walks framework.[8–15]

In this paper, we address the problem of optimally routing an excitation between two different possible target sites on the simplest graph apt to this task with chiral quantum walks. We make connections with spin chains, and we also provide an alternative way to transport quantum information exploiting just the degrees of freedom of

the quantum walk.[16–24] This allows us to significantly reduce the dimensionality of the underlying Hilbert space with respect to a spin chain, thus improving the resilience to decoherence. We also address the robustness of transport with respect to optimal values of the phase and analyze in some detail the characterization of the router, i.e., the problem of estimating the value of the phase by quantum probing. It is also relevant to notice that proposals for experimental implementations of chiral quantum walks, on graphs of the same type as the one discussed here, have been put forward recently.[25]

The paper is structured as follows. In Sec. II, we establish notation and recall some elements of the theory of continuous-time chiral quantum walks. In Sec. III, we introduce the system studied in this work and present our results about routing of classical and quantum information. Section IV is devoted to the characterization of the quantum router, whereas Sec. V closes the paper with some concluding remarks.

II. CONTINUOUS-TIME CHIRAL QUANTUM WALKS

Let us start by introducing the notation that will be used during the rest of the work. Starting from a connected simple graph G(V,E), where $V = \{1, \ldots, N\}$ with $N = |V|$ specifies the vertices and E the connections, we define the site basis $\{|1\rangle, \ldots, |N\rangle\}$ such that $\langle i|j\rangle = \delta_{ij}$, $i, j = 1, \ldots, N$. Each element $|i\rangle$ of the basis represents a state localized on the vertex i. Given an initial state $|\psi\rangle$, a continuous-time quantum walk (CTQW) is defined as the time evolution of the state through a unitary operator $U = e^{-iHt}$, where H is a suitable Hamiltonian that satisfies the topology of the graph, usually assumed to be the Laplacian or the adjacency matrix of the graph. Those choices, however, do not allow for directional transport of the excitation because the Hamiltonian is a real matrix and any transition probability $|\langle j|e^{-iHt}|k\rangle|^2$ is symmetric under the exchange $j \leftrightarrow k$. In order to overcome these limits and discuss directionality of quantum transport, one should assume a complex Hermitian Hamiltonian corresponding to chiral quantum walks, which themselves stand out as the simplest generalization to introduce routing in a quantum walks framework.[11]

Earlier works about chiral quantum walks[8,9] assumed some specific form of chiral Hamiltonians, without referring to specific systems where such interactions may take place. A systematic approach to chiral quantum walks has been then put forward in Ref. 11, introducing a full characterization of all the possible Hamiltonians describing the time evolution over a given topology. The elements of those Hamiltonians satisfy the relations $L_{ij} = H_{ii}^2\delta_{ij} - |H_{ij}|^2$, where L is the Laplacian of the graph. This set of equations has an infinite number of solutions (i.e., of valid Hamiltonians), which are of the form

$$H = \sum_{j\neq k\in E} \left[e^{i\theta_{jk}}|j\rangle\langle k| + e^{-i\theta_{jk}}|k\rangle\langle j|\right] + \sum_{s=1}^{N}\gamma_s|s\rangle\langle s|, \tag{1}$$

where the off-diagonal phases θ_{jk} and the diagonal self-energies γ_s are free parameters not determined by the sole topology.

A. A remark on the number of independent phases

Among the infinite number of Hamiltonians that are compatible with a given topology, those with a given set of self-energies $\{\gamma_s\}$ may be transformed one to each other by unitary transformations U that acts diagonally on the site basis, i.e.,

$$U|j\rangle = e^{i\phi_j}|j\rangle \quad j = 1, \ldots, N. \tag{2}$$

Applying a transformation of this kind to a given Hamiltonian, the off-diagonal phases θ_{jk} are mapped to $\theta'_{jk} = \theta_{jk} + (\phi_j - \phi_k)$. This class of transformations changes the transition amplitudes from a site to another but do not affect the site-to-site transition probabilities $|\langle j|e^{-iHt}|k\rangle|^2$, as it may be easily seen from

$$\begin{aligned} |\langle j|e^{-iH't}|k\rangle|^2 &= |\langle j|U^\dagger e^{-iHt}U|k\rangle|^2 \\ &= |e^{i(\phi_j-\phi_k)}\langle j|e^{-iHt}|k\rangle|^2 \\ &= |\langle j|e^{-iHt}|k\rangle|^2. \end{aligned} \tag{3}$$

In other words, if one is interested only in the site-to-site transition probabilities, the set of possible Hamiltonians naturally splits into equivalence classes, and one may employ the most convenient representative by re-phasing sites via a unitary transformation of the form (2). This also means that if the quantities of interest are the site-to-site transition probabilities, the number of independent parameters (phases) at disposal to engineer the dynamics is smaller than the number of nonzero off-diagonal elements.

Let us now introduce the total phase along a loop of the graph as $\Theta \equiv \sum_{j\neq k}\theta_{jk}$, where the sum is performed over the links defining the loop. Using Eq. (2), it is easy to see that this quantity is invariant under site re-phasing, i.e., $\Theta' = \sum_{j\neq k}\theta'_{jk} = \Theta$. This means that for graphs with no loops, e.g., any tree graph, the transition probabilities cannot be changed using complex Hamiltonians (since all the off-diagonal phases may be removed by re-phasing). On the other hand, in graphs with loops, the number of free phases at disposal to engineer the transition probabilities (e.g., to obtain directionality) is equal to the number of loops. As we will see in Sec. III, chiral effects induced by off-diagonal phases are enough to obtain quantum routing of information even in graphs with a single loop.

III. THE QUANTUM ROUTER

Routing is a fundamental function of any network, classical or quantum. Indeed, networks where information travels across different devices have to be equipped with a means of selecting paths through the network itself.[26,27]

The goal of this section is to show how a nearly optimal *quantum router* may be built using chiral quantum walk on a simple graph. In particular, we consider the minimal structure depicted in Fig. 1 and show that by tuning the single parameter $\Theta \equiv \theta$, one may route an excitation initially located at site $|1\rangle$ to site $|5\rangle$ or $|6\rangle$ with high probability. This task is not possible with standard (i.e., non chiral) quantum walk, whereas by exploiting chirality, one may achieve transport with probability very close to unit. In addition, we show that routing and nearly optimal transport are also possible for an excitation initially prepared in superposition, i.e., any superposition of the form $|\psi\rangle \propto |1\rangle + e^{i\phi}|2\rangle$ may be sent with high fidelity to $|\psi\rangle \propto |5\rangle + e^{i\phi}|3\rangle$ or to $|\psi\rangle \propto |6\rangle + e^{i\phi}|4\rangle$ by tuning the phase θ.

The schematic diagram of our chirality-based minimal-topology quantum router is shown in Fig. 1. Vertex labels are those used

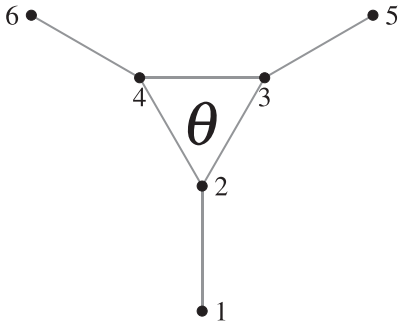

FIG. 1. Schematic diagram of a chirality-based minimal-topology quantum router. Vertex labels are those used in the main text. The overall Hamiltonian of the quantum walker is parametrized by the total phase along the loop, denoted by θ, and by the difference $\gamma \equiv \gamma_{int} - \gamma_{ext}$ among the self-energies of the internal and external links.

throughout the paper. Among the possible *bona fide* chiral Hamiltonians of the form (1), we focus on those with

$$\begin{aligned} \gamma_j &= \gamma_{int} \quad \text{for } j = 2,3,4, \\ \gamma_j &= \gamma_{ext} \quad \text{for } j = 1,5,6, \\ \theta_{ij} &= 0 \quad \text{for the links outside the loop}, \\ \theta_{ij} &= \theta/3 \quad \text{for links along the loop}. \end{aligned}$$

With this choice, we ensure that the rotational symmetry of the graph is preserved, and that the only relevant phase is the total phase $\Theta \equiv \theta$ along the loop. These features make the structure in Fig. 1 an ideal candidate to route quantum information and, at the same time, maintain the problem analytically treatable.

We now notice that the site-to-site transition probabilities do not change if we consider a modified Hamiltonian where a term proportional to the identity, e.g., $\gamma_{ext}\mathrm{I}$, is added (subtracted). This reveals that only the difference $\gamma \equiv \gamma_{int} - \gamma_{ext}$ is relevant for engineering the dynamics. We, thus, consider the effective Hamiltonian $H \to H - \gamma_{ext}\mathrm{I}$. The explicit form is given by $H = |1\rangle\langle 2| + e^{i\frac{\theta}{3}}|2\rangle\langle 3| + e^{-i\frac{\theta}{3}}|2\rangle\langle 4| + e^{i\frac{\theta}{3}}|3\rangle\langle 4| + |3\rangle\langle 5| + |4\rangle\langle 6| + h.c. + \gamma(|2\rangle\langle 2| + |3\rangle\langle 3| + |3\rangle\langle 4|)$ or, in matrix form, by

$$H = \begin{bmatrix} 0 & 1 & 0 & 0 & 0 & 0 \\ 1 & \gamma & e^{-i\frac{\theta}{3}} & e^{i\frac{\theta}{3}} & 0 & 0 \\ 0 & e^{i\frac{\theta}{3}} & \gamma & e^{-i\frac{\theta}{3}} & 1 & 0 \\ 0 & e^{-i\frac{\theta}{3}} & e^{i\frac{\theta}{3}} & \gamma & 0 & 1 \\ 0 & 0 & 1 & 0 & 0 & 0 \\ 0 & 0 & 0 & 1 & 0 & 0 \end{bmatrix}. \tag{4}$$

This Hamiltonian reflects the rotational symmetry of the graph, and we may, thus, assume that its eigenstates satisfy the relations

$$\begin{aligned} \langle E_n|k_{int}\rangle &= e^{i\frac{2\pi k(n-1)}{3}}\alpha, \\ \langle E_n|k_{ext}\rangle &= e^{i\frac{2\pi k(n-1)}{3}}\beta, \end{aligned} \tag{5}$$

where α and β are real numbers, $n = 1, \ldots, 6$, and $|k\rangle$ with $k_{int} = 2,3,4$ and $k_{ext} = 1,6,5$ denotes localized states. Using this ansatz, the eigenvalues of the Hamiltonian are easily found as

$$E_n = S_n + (-1)^{\mathrm{mod}(n,2)}\sqrt{1+S_n^2}, \tag{6}$$

$$S_n = \frac{\gamma}{2} + \cos\left[\frac{\theta}{3} + \frac{4\pi}{3}\mathrm{mod}(n-1,3)\right]. \tag{7}$$

The eigenvalues are shown as a function of θ in Fig. 2 for $\gamma = 0,1,2$. For increasing γ, the three negative eigenvalues tend to coalesce and vanish as $-1/\gamma$, whereas the three positive ones increase their magnitudes. For negative values of γ, the behavior of negative and positive eigenvalues is reversed.

The corresponding eigenvectors are given by

$$|E_n\rangle = \frac{1}{\sqrt{3(1+E_n^2)}}\begin{pmatrix} 1 \\ E_n \\ e^{i\frac{2\pi(n-1)}{3}}E_n \\ e^{i\frac{4\pi(n-1)}{3}}E_n \\ e^{i\frac{2\pi(n-1)}{3}} \\ e^{i\frac{4\pi(n-1)}{3}} \end{pmatrix}. \tag{8}$$

Notice that given the parametrization of the Hamiltonian in Eq. (4), in order to obtain all possible values for the phases on the links, the phase parameter should take values in the interval $\theta \in [0, 6\pi)$. However,

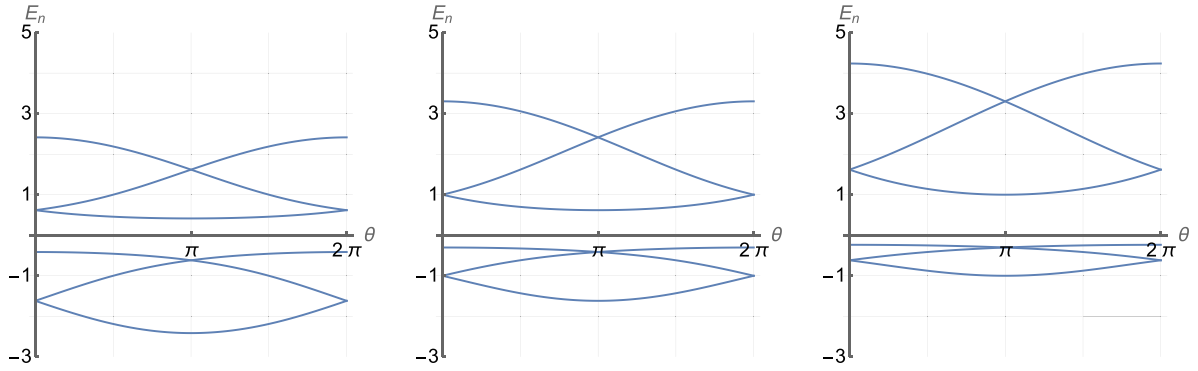

FIG. 2. Eigenvalues of H as a function of θ for $\gamma = 0,1,2$ (from left to right).

since the total phase is the only relevant parameter to engineer the transition probabilities, it is sufficient to consider $\theta \in [0, 2\pi)$ in order to design a quantum router. Notice also that if one prepares the walker in an eigenstate, the ratio between the probability of being localized inside or outside of the loop is given by

$$R_n(\theta) \equiv \frac{\sum_{j=2,3,4} |\langle j|E_n\rangle|^2}{\sum_{j=1,5,6} |\langle j|E_n\rangle|^2} = E_n^2, \tag{9}$$

which means that one may estimate the energy of the eigenstate upon estimating this probability ratio by measuring a dichotomic *in–out* observable.

Let us now address the main topic of the paper, i.e., how to exploit chirality to obtain directionality and, in turn, the effective routing of classical and quantum information. We start by considering a walker initially localized in one of the external sites, say $|1\rangle$, and analyze the probability of being transferred to one of the other outer states, i.e., $|5\rangle$ or $|6\rangle$ at some time t. As we will see, it is, indeed, possible to achieve nearly perfect routing, that is, one may choose where to route the walker by tuning θ and obtain a transition probability very close to one for short time evolution, i.e., for instants of time reasonably short compared to the energy gaps of the system.

Upon expanding the unitary evolution operator $U = e^{-iHt} = \sum_n e^{-iE_n t}|E_n\rangle\langle E_n|$ and using Eqs. (6) and (8), we obtain

$$P_{15}(t,\theta,\gamma) = \left| \sum_{n=1}^{6} e^{-iE_n t} \frac{e^{-i\frac{2\pi}{3}(n-1)}}{3(1+E_n^2)} \right|^2, \tag{10}$$

$$P_{16}(t,\theta,\gamma) = \left| \sum_{n=1}^{6} e^{-iE_n t} \frac{e^{-i\frac{4\pi}{3}(n-1)}}{3(1+E_n^2)} \right|^2. \tag{11}$$

Both expressions are analytic, but it is not easy to understand their general behavior due to the high number of oscillating terms. In order to gain more insight about their properties, we illustrate the behavior of $P_{15}(t,\theta) \equiv P_{15}(t,\theta,\gamma \equiv 0)$ and $P_{16}(t,\theta) \equiv P_{16}(t,\theta,\gamma \equiv 0)$ as a function of time and the total phase in Fig. 3. As it is apparent from the plots, there are instants of time when one may switch from the situation $P_{15} \simeq 1$, $P_{16} \simeq 0$ to $P_{15} \simeq 0$, $P_{16} \simeq 1$ by tuning the total phase θ. In other words, one may *route* the excitation from site 1 to site 5 or from site 1 to site 6 just by tuning the parameter θ (which itself may be tuned using an external field).

Upon maximizing $P_{15}(t,\theta)$ over θ at fixed t (or equivalently P_{16}) and exploiting the symmetry $P_{15}(t,\theta) = P_{16}(t, 2\pi - \theta)$, one obtains the optimal values for the routing phase, which turns out to be $\theta = \pi/2, 3/2\pi$. This is illustrated in Fig. 4, where we show $P_{15}(t,\theta)$, $P_{16}(t,\theta)$ and their sum as a function of θ for two specific values of the interaction time.

The routing effect is apparent from the plots. Setting the total phase to the optimal value, we have $P_{15} \gg P_{16}$, or vice-versa, and also have $P_{15} + P_{16} \simeq 1$, i.e., the excitation is effectively routed to the other outer sites, without being trapped in the loop of the graph (we have $P_{15} + P_{16} \simeq 0.88$ at $t^* = 2.629$ and $P_{15} + P_{16} \simeq 0.97$ at $t^* = 18.95$). It is also remarkable that the effect appears at multiple instants of time (which we refer to as t^*), meaning that routing may be implemented with structures and platforms of different sizes. However, for those larger values of t^*, the probability peaks are sharper, i.e., the routing

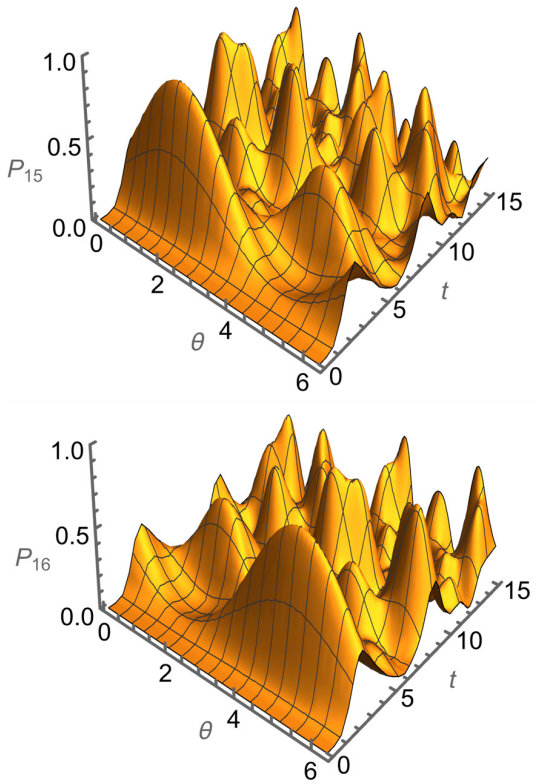

FIG. 3. The transition probabilities $P_{15}(t,\theta)$ (upper panel) and $P_{16}(t,\theta)$ (lower panel) as a function of the interaction time t and the total phase θ.

effects are less robust. Overall, we have a trade-off between the routing effectiveness and its robustness, making the first values of t^* more convenient for practical applications. Notice that for $\theta = \pi/2$, the probability P_{15} may be written as $P_{15}(t,\pi/2) = \frac{4}{9}f(t)^2$, where $f(t)$ is a real function reported in the Appendix. An analogue result may be found for $P_{16}(t,\pi/2)$.

Finally, we remark that the quantum router described in this section has been designed setting $\gamma = 0$, i.e., using only the chiral nature of the Hamiltonian and without exploiting the degree of freedom offered by the onsite energies. However, since the Hamiltonian in Eq. (4) also depends on the diagonal elements, one may wonder about their potential role in routing information. Investigating the probabilities numerically, we found that by setting $\gamma \neq 0$, one may enhance routing (i.e., the two probabilities are closer to 1 and 0, respectively) though the optimal phase and interaction time, which are no longer the same.

In other words, we have $P_{15}(t^*,\pi/2,\gamma)/P_{15}(t^*,\pi/2,0) < 1$ and $P_{16}(t^*,\pi/2,\gamma)/P_{16}(t^*,\pi/2,0) > 1 \forall\gamma$, where t^* is one of the optimal values of time discussed earlier, but we may find other values of the parameters, say t_M, θ_M, and γ_M for which $P_{15}(t_M,\theta_M,\gamma_M)/P_{15}(t^*,\pi/2,0) > 1$ and $P_{16}(t_M,\theta_M,\gamma_M)/P_{16}(t^*,\pi/2,0) < 1$. The two effects are illustrated in the two panels of Fig. 5. In the upper panel, we show $P_{15}(t^*,\pi/2,\gamma)$ and $P_{16}(t^*,\pi/2,\gamma)$ as a function of γ

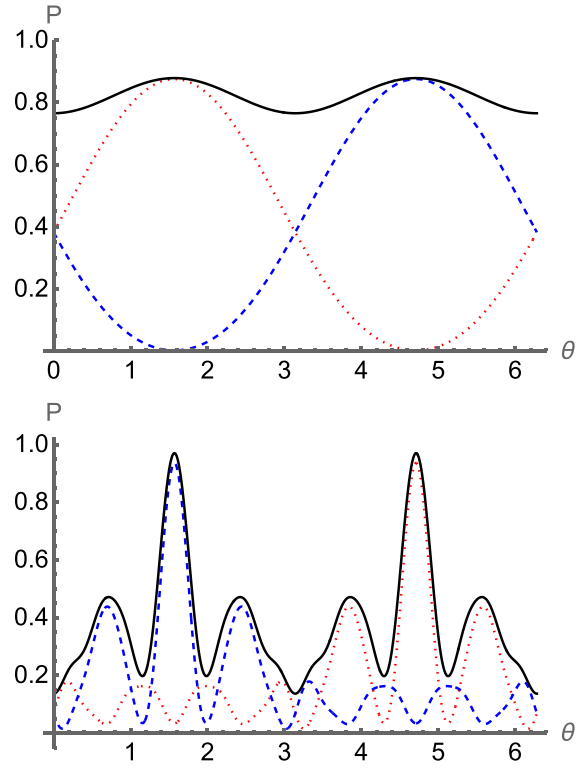

FIG. 4. The transition probabilities $P_{15}(t,\theta)$ (dotted red) and $P_{16}(t,\theta)$ (dashed blue), together with their sum (solid black) as a function of θ for $t=2.629$ (upper panel) and $t=18.95$ (lower panel). Notice that for $t=2.629$, we have nearly perfect routing $1\to 5$ for $\theta=\pi/2$ and $1\to 6$ for $\theta=3\pi/2$, whereas for $t=18.95$, the two phases are switched.

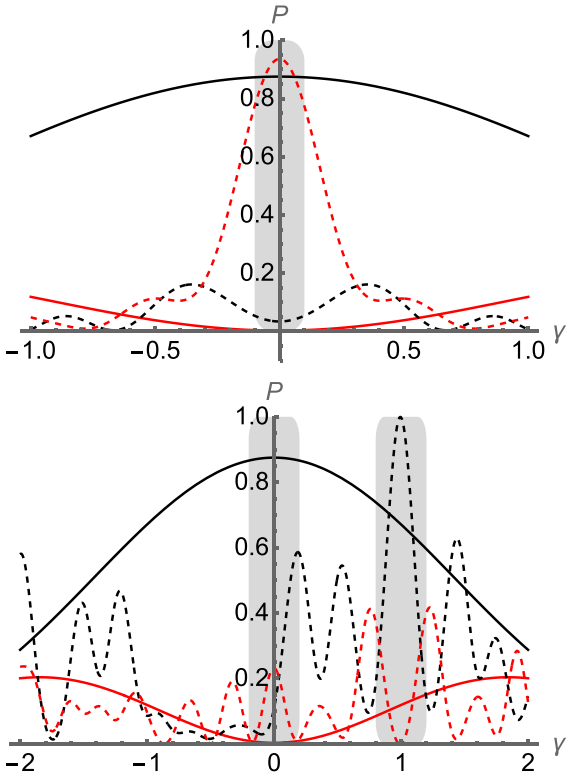

FIG. 5. (Top) The transitions probabilities $P_{15}(t^*,\pi/2,\gamma)$ (black) and $P_{16}(t^*,\pi/2,\gamma)$ (red) as a function of γ for $t^*=2.629$ (solid) and $t^*=18.95$ (dashed). (Bottom) $P_{15}(2.629,\pi/2,\gamma)$ (solid black) and $P_{16}(2.629,\pi/2,\gamma)$ (solid red) as a function of γ, compared to $P_{15}(t_M,\theta_M,\gamma)$ (dashed black) and $P_{16}(t_M,\theta_M,\gamma)$ (dashed red) with $t_M\simeq 31.4$ and $\theta_M\simeq 0.11$. The gray regions highlight where the routing effect is taking place.

for the two values of t^* mentioned earlier. As it is apparent from the plot, for $\gamma\neq 0$, the performance of the system as a router gets worse (see the region highlighted in gray). In the lower panel, we instead compare $P_{15}(t^*,\pi/2,\gamma)$ and $P_{16}(t^*,\pi/2,\gamma)$ to $P_{15}(t_M,\theta_M,\gamma)$ and $P_{16}(t_M,\theta_M,\gamma)$ with $t_M\simeq 31.4$ and $\theta_M\simeq 0.11$. In this case, the optimal values of γ are different (they are $\gamma=0$ and $\gamma=1$, respectively, see the gray regions), and the $\gamma\neq 0$ case provides a more effecting routing effect.

Let us now address the routing of quantum information, i.e., of states exhibiting coherence in the site basis. In particular, we consider an excitation initially de-localized over the sites $|1\rangle$ and $|2\rangle$, i.e., prepared in a generic superposition of the form

$$|\phi_{12}\rangle=\frac{|1\rangle+e^{i\phi}|2\rangle}{\sqrt{2}},$$

and investigate the possibility of routing the state to the analogue superpositions of sites $|5\rangle$ and $|3\rangle$ or $|6\rangle$ and $|4\rangle$, i.e., the states

$$|\phi_{53}\rangle=\frac{|5\rangle+e^{i\phi}|3\rangle}{\sqrt{2}},$$
$$|\phi_{64}\rangle=\frac{|6\rangle+e^{i\phi}|4\rangle}{\sqrt{2}}.$$

As we will see, routing of quantum information is, indeed, possible, and it is even possible to design a universal quantum router, able to route any superposition of the form $|\phi_{12}\rangle$, independently on the value of the superposition phase ϕ. We set $\gamma=0$ and denote the transition probabilities $|\langle\phi_{53}|U|\phi_{12}\rangle|^2$ and $|\langle\phi_{64}|U|\phi_{12}\rangle|^2$ by $P_R(t,\theta,\phi)$ and $P_L(t,\theta,\phi)$, respectively.

Using the relations

$$\partial_t\langle 1|U|5\rangle=-i\langle 1|UH|5\rangle=-i\langle 1|U|3\rangle,$$
$$\partial_t\langle 1|U|5\rangle=-\langle 1|HU|5\rangle=-i\langle 2|U|5\rangle,$$
$$\partial_{tt}\langle 1|U|5\rangle=-\langle 1|HUH|5\rangle=-\langle 2|U|3\rangle,$$

we may write

$$P_R(t,\theta,\phi)=\frac{1}{4}|\langle 1|U|5\rangle+2i\cos\phi\,\partial_t\langle 1|U|5\rangle-\partial_{tt}\langle 1|U|5\rangle|^2. \quad (12)$$

In particular, for $\theta=\frac{\pi}{2}$, we have

$$P_R\left(t,\frac{\pi}{2},\phi\right)=\frac{1}{4}|f(t)+2i\cos\phi\,\partial_t f(t)-\partial_{tt}f(t)|^2, \quad (13)$$

where $f(t)$ is reported in the Appendix.

The dependence on the superposition phase ϕ is multiplied by the time derivative of the amplitude $\langle 1|U|5\rangle$. When this derivative is zero (notice that $\langle 1|U|5\rangle$ is a complex number), the transport probability is independent on ϕ, i.e., it is the same for all the superposition states of the form $|\phi_{12}\rangle$. For those instants of time t^*, the value of the transport probability is

$$P_R\left(t^*, \frac{\pi}{2}, \phi\right) = \frac{1}{4}|f(t^*) - \partial_{tt} f(t)|_{t=t^*}|^2. \tag{14}$$

The first value is $t^* = 2.629$ and coincides with the first instant of time optimizing routing for localized states. It corresponds to $P_R\left(t^*, \frac{\pi}{2}, \phi\right) = 0.83$. Upon sending θ into $2\pi - \theta$, the same line of reasoning may be applied to $P_L\left(t^*, \frac{\pi}{2}, \phi\right)$.

We should remark that the aforementioned setting makes the probability ϕ-independent but not necessarily optimal for all the value of ϕ. If the value of ϕ is fixed, a specific optimization may be done separately. Notice, however, that the differences are not dramatic, and that the instants of time optimizing the routing for localized states are also *pretty good*[28,29] for all superpositions. This is illustrated in Fig. 6, where we show $P_R\left(t, \frac{\pi}{2}, \phi\right)$ for different values of ϕ. The gray areas highlight the region around $t^* = 2.629$ (light gray), where universality occurs, and the interval $t \in [2.35, 2.55]$ (dark gray), where the maxima for the considered values of ϕ are found.

Finally, we emphasize once again that chirality is a crucial ingredient to achieve the universal routing of superpositions, which would not be possible for a non-chiral CTQW, since in that case $\theta = 0$.

IV. PROBING THE ROUTER PHASE

As we have illustrated in Sec. III, the structure in Fig. 1, when equipped with the Hamiltonian in Eq. (4), allows one to route classical and quantum information by tuning (and switching) θ, i.e., the total phase that the walker acquires along the loop. The routing effect appears *robust* since the peaks in Fig. 4 are *broad* compared to the range of variation of θ. However, this is only a qualitative assessment, and a proper benchmark for robustness may be obtained only by comparing those widths to the uncertainty in determining the value of θ for a given physical platform. A question, thus, naturally arises about the ultimate precision achievable in estimating the total phase by probing the router. This problem may be addressed by the tools of quantum estimation theory[30,31] and quantum probing.[32–37] A natural characterization scheme is the following: the walker is repeatedly prepared in a known state $|\psi_0\rangle$ and is let to evolve on the graph for a given interval of time. Then, an observable X is measured, and a set of M outcomes $\{x_1, x_2, \ldots, x_M\}$ is collected. Data are distributed according to the conditional distribution $p(x|\theta, t) = |\langle x|U|\psi_0\rangle|^2$, and the value of θ is inferred using an *estimator* $\bar{\theta} \equiv \bar{\theta}(\{x_1, x_2, \ldots, x_M\})$, i.e., a function of data.

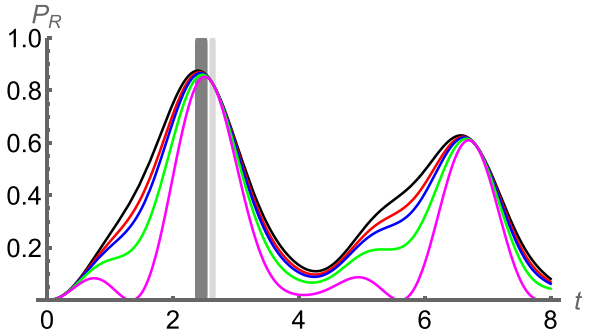

FIG. 6. The $12 \to 53$ transition probability $P_R\left(t, \frac{\pi}{2}, \phi\right)$ as a function of the interaction time for different values of $\phi = 0, \pi/8, \pi/6, \pi/4$, and $\pi/2$ (black, red, blue, green, and magenta, respectively). The light gray area highlights the region around $t^* = 2.629$, and the dark gray one the interval $t \in [2.35, 2.55]$ (see the text).

The ultimate bound on the precision achievable by any procedure of this kind (i.e., the precision achievable by optimizing over all the observables and all the possible estimators) is bounded by the quantum Cramèr–Rao bound $\mathrm{Var}\bar{\theta} \geq [MQ(\theta)]^{-1}$, where $Q(\theta)$ is the quantum Fisher information (QFI) of the family of states $|\psi_\theta\rangle = U|\psi_0\rangle$ (usually referred to as a *quantum statistical model*). In our case, the QFI is given by[38]

$$Q(\theta) = 4\langle\psi_0|\Delta\mathscr{H}^2|\psi_0\rangle = 4\left(\langle\psi_0|\mathscr{H}^2|\psi_0\rangle - \langle\psi_0|\mathscr{H}|\psi_0\rangle^2\right), \tag{15}$$

where

$$\mathscr{H} = -i\left(\partial_\theta U^\dagger\right)U. \tag{16}$$

Notice that $\mathscr{H} \neq H$ since the dependence of the evolution operator U on the parameter θ is non trivial (we would have $\mathscr{H} = H$ for and evolution operator of the form $U = e^{-iH\theta}$). Optimized quantum probes to characterize the router are, thus, initial preparations $|\psi_0\rangle$ maximizing the QFI in Eq. (15). Given the unitary nature of the map $|\psi_0\rangle \to |\psi_\theta\rangle$, we expect the QFI to grow asymptotically (i.e., for $t \gg 1$) as $Q(\theta) = \kappa(\theta)\, t^2$ for all initial states,[38–40] with optimal probes maximizing $\kappa(\theta)$. Actually, we have not performed an optimization over all possible initial preparations but rather compared the QFI obtained for some specific initial preparations, chosen because they are likely to be easily prepared on physical platforms.

In the upper panel of Fig. 7, we show the function $\kappa(\theta)$ as a function of θ for the localized states $|\psi_0\rangle = |1\rangle$ (blue dotted) and $|\psi_0\rangle = |2\rangle$ (the upper red curve), and for the *flat* superposition $|\psi_0\rangle = \frac{1}{\sqrt{6}}\sum_{j=1}^{6}|j\rangle$ (the lower black dashed curve, nearly indistinguishable from the x-axes). Results for the other outer and inner localized states are the same. The most convenient setting is, thus, to prepare the walker in a localized state on one of the sites of the loop and let it evolves as long as possible. In the lower panel of Fig. 7, we illustrate the influence of self-energies, i.e., what happens for $\gamma \neq 0$. In particular, we show the behavior of the QFI for $|\psi_0\rangle = |2\rangle$. Upon increasing γ, the QFI increases and its dependence on θ weakens. For large γ, we have the asymptotic results $\kappa = 8/3\, t^2(1/3 - 1/\gamma^2)$, independently on θ, a result that may also obtained analytically by expanding the eigenvalues and the eigenvectors of the Hamiltonian at the leading order in γ. In order to achieve the earlier precision, one has to measure an optimal observable, which is given by the so-called symmetric logarithmic derivative (SLD) $L = 2i[\mathscr{H}, |\psi_0\rangle\langle\psi_0|]$.[38] In our case, the SLD at first order in $1/\gamma$ may be written as

$$L = \frac{2}{3}t\left[e^{-i\frac{\theta}{3}}|2\rangle\langle 3| + e^{i\frac{\theta}{3}}|2\rangle\langle 4| + \frac{1}{\gamma}\left(e^{-i\frac{\theta}{3}}|2\rangle\langle 5| + e^{-i\frac{\theta}{3}}|2\rangle\langle 6|\right)\right] + h.c.$$

The form is remarkably simple and emphasizes that for large γ, only the internal sites are involved. However, the possibility of implementing the measurement of this observable in practice strongly depends on the platform under investigation.

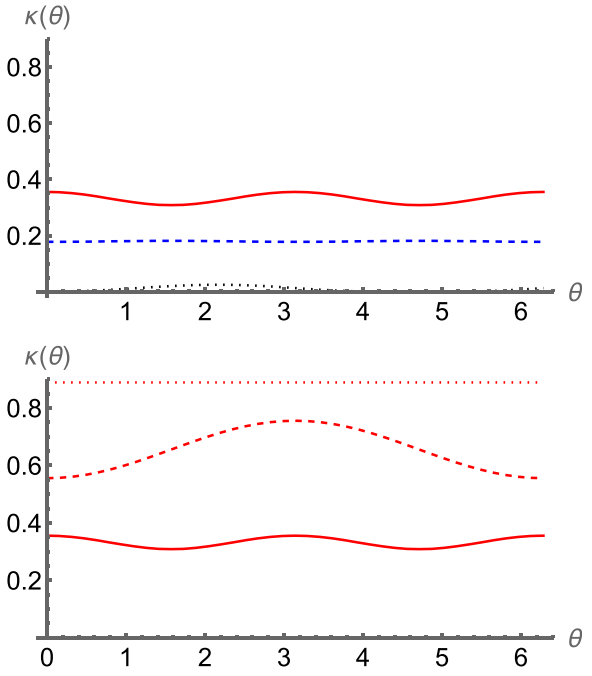

FIG. 7. (Top) The function $\kappa(\theta) \overset{t\gg 1}{\equiv} Q(\theta)/t^2$ as a function of θ for $|\psi_0\rangle = |1\rangle$ (blue dotted), $|\psi_0\rangle = |2\rangle$ (the upper red curve), and $|\psi_0\rangle = \frac{1}{\sqrt{6}}\sum_{j=1}^{6}|j\rangle$ (black dashed, nearly indistinguishable from the x-axes). (Bottom) The function $\kappa(\theta)$ as a function of θ for $|\psi_0\rangle = |2\rangle$ and $\gamma = 0$ (solid), $\gamma = 3$ (dashed), and $\gamma = 7$ (dotted).

It is also instructive to investigate whether some information about the value of the total phase may be inferred by measuring the position of the walker after propagation. Given a walker initially prepared in the state $|\psi_0\rangle$, the time-dependent probability of detecting the walker at site j after the interaction time t is given by $q(j,t|\theta,\psi_0) = |\langle j|U|\psi_0\rangle|^2$. The corresponding Fisher information is given by $F(\theta,t|\psi_0) = \sum_{j=1}^{6}[\partial_\theta\, q(j,t|\theta,\psi_0)]^2/q(j,t|\theta,\psi_0)$. The Fisher information shows many oscillations and strongly depends on time and on the actual value of the total phase. Remarkably, though, it vanishes at any time $F(\pm\pi/2,t||1\rangle) = 0$ if the initial state corresponds to a walker localized in the first site $|\psi_0\rangle = |1\rangle$, and the total phase is $\theta = \pm\pi/2$, i.e., the configurations used to build the quantum router. Physically, this means that in this regime, it is not possible to extract information about the total phase looking at the position of the walker. In other words, fluctuations in the total phase around the values $\theta = \pm\pi/2$ do not lead to detectable changes at the output, i.e., the routing effects are robust against fluctuations of the total phase. This is confirmed by the fact that $F(\pm\pi/2,t|\psi_0) = 0$ vanishes also for $|\psi_0\rangle = |2\rangle$ and $|\psi_0\rangle = (|1\rangle + |2\rangle)/\sqrt{2}$ and for larger values of γ.

V. CONCLUSIONS

We have addressed the use of chiral quantum walks to route classical and quantum information over quantum network. In particular, we have shown that using a minimal graph structure is enough to model directional transfer of information over a network. Upon tuning the total phase along the loop of the graph, high-fidelity routing and transport are possible for localized states and coherent superpositions of them. Furthermore, we have shown how to achieve universal quantum routing with fidelity independent on the input state. In our scheme, chirality is governed by a single phase, and the routing probability is robust against fluctuations of this parameter. Finally, we have addressed characterization of quantum routers and evaluated the quantum Fisher information for different quantum probes, also showing how to exploit the self-energies of the graph to achieve high precision in estimating the phase parameter. We have also proved the robustness of the routing effect against fluctuations of the total phase.

Our results confirm that chiral quantum walks represent a useful resource to design quantum information protocols over networks and pave the way to the design of larger structures to test whether chirality may be exploited to route information in multiple directions. In particular, a question arises on whether the basic triangular router analyzed in this work is still optimal for multiple routing, or larger structures with possibly more free phases are required.

ACKNOWLEDGMENTS

This work was performed under the auspices of GNFM-INdAM. M.G.A.P. thanks Claudia Benedetti, Alessandro Candeloro, and Emilio Annoni for useful discussions.

AUTHOR DECLARATIONS

Conflict of Interest

The authors have no conflicts to disclose.

Author Contributions

Alberto Bottarelli: Investigation (equal); Writing – original draft (equal). **Massimo Frigerio:** Conceptualization (equal); Formal analysis (equal); Investigation (equal); Methodology (equal); Supervision (equal); Validation (equal); Writing – review & editing (equal). **Matteo G. A. Paris:** Conceptualization (lead); Data curation (equal); Formal analysis (equal); Investigation (equal); Methodology (equal); Project administration (lead); Software (equal); Supervision (lead); Validation (lead); Visualization (lead); Writing – review & editing (lead).

DATA AVAILABILITY

The data that support the findings of this study are available from the corresponding author upon reasonable request.

APPENDIX: THE FUNCTION F(T) IN EQ. (13)

The function $f(t) = f_r(t) + if_i(t)$ is given by

$$f_r(t) = \frac{\sin\left(\frac{\sqrt{3}t}{2}\right)\sin\left(\frac{\sqrt{7}t}{2}\right)}{2\sqrt{21}} - \frac{\cos(t)}{6} + \frac{1}{6}\cos\left(\frac{\sqrt{3}t}{2}\right)\cos\left(\frac{\sqrt{7}t}{2}\right) - \frac{\sin\left(\frac{\sqrt{3}t}{2}\right)\cos\left(\frac{\sqrt{7}t}{2}\right)}{2\sqrt{3}} + \frac{\sin\left(\frac{\sqrt{7}t}{2}\right)\cos\left(\frac{\sqrt{3}t}{2}\right)}{2\sqrt{7}}, \quad \text{(A1)}$$

$$f_i(t) = \frac{\sin\left(\frac{\sqrt{3}t}{2}\right)\sin\left(\frac{\sqrt{7}t}{2}\right)}{2\sqrt{7}} - \frac{\cos(t)}{2\sqrt{3}} + \frac{\cos\left(\frac{\sqrt{3}t}{2}\right)\cos\left(\frac{\sqrt{7}t}{2}\right)}{2\sqrt{3}} - \frac{1}{2}\sin\left(\frac{\sqrt{3}t}{2}\right)\cos\left(\frac{\sqrt{7}t}{2}\right) + \frac{1}{2}\sqrt{\frac{3}{7}}\sin\left(\frac{\sqrt{7}t}{2}\right)\cos\left(\frac{\sqrt{3}t}{2}\right). \quad \text{(A2)}$$

REFERENCES

[1] M. Ahumada, P. A. Orellana, F. Domínguez-Adame, and A. V. Malyshev, Phys. Rev. A **99**, 033827 (2019).
[2] S. Bose, Phys. Rev. Lett. **91**, 207901 (2003).
[3] S. Paganelli, S. Lorenzo, T. J. Apollaro, F. Plastina, and G. L. Giorgi, Phys. Rev. A **87**, 062309 (2013).
[4] B. Chen, Y.-Z. He, T.-T. Chu, Q.-H. Shen, J.-M. Zhang, and Y.-D. Peng, Prog. Theor. Exp. Phys. **2020**, 053A01.
[5] O. Mülken and A. Blumen, Phys. Rep. **502**, 37 (2011).
[6] S. E. Venegas-Andraca, Quantum Inf. Process. **11**, 1015 (2012).
[7] R. Portugal, *Quantum Walks and Search Algorithms* (Springer, 2013), Vol. 19.
[8] Z. Zimborás, M. Faccin, Z. Kadar, J. D. Whitfield, B. P. Lanyon, and J. Biamonte, Sci. Rep. **3**, 2361 (2013).
[9] D. Lu, J. D. Biamonte, J. Li, H. Li, T. H. Johnson, V. Bergholm, M. Faccin, Z. Zimborás, R. Laflamme *et al.*, Phys. Rev. A **93**, 042302 (2016).
[10] A. Sett, H. Pan, P. Falloon, and J. Wang, Quantum Inf. Process. **18**, 159 (2019).
[11] M. Frigerio, C. Benedetti, S. Olivares, and M. G. A. Paris, Phys. Rev. A **104**, L030201 (2021).
[12] A. Khalique, A. Sett, J. Wang, and J. Twamley, New J. Phys. **23**, 083005 (2021).
[13] M. Frigerio, C. Benedetti, S. Olivares, and M. G. A. Paris, Phys. Rev. A **105**, 032425 (2022).
[14] U. Sağlam, M. Paternostro, and Ö. E. Müstecapl ioğlu, Physica A **612**, 128480 (2023).
[15] R. Chaves, B. Chagas, and G. Coutinho, Quantum Inf. Process. **22**, 41 (2023).
[16] P. Høyer and J. Leahy, Phys. Rev. A **106**, 022418 (2022).
[17] S. Skoupý and M. Štefaňák, Phys. Rev. A **103**, 042222 (2021).
[18] T. Wong, Phys. Rev. A **100**, 062325 (2019).
[19] H.-J. Li, X.-B. Chen, Y.-L. Wang, Y.-Y. Hou, and J. Li, Quantum Inf. Process. **18**, 266 (2019).
[20] X. Li, H. Chen, Y. Ruan, Z. Liu, and W. Liu, Quantum Inf. Process. **18**, 195 (2019).
[21] T. Wong, J. Phys. A **50**, 475301 (2017).
[22] G. Berkolaiko, H. Schanz, and R. Whitney, Phys. Rev. Lett. **88**, 104101 (2002).
[23] P. Exner, M. Tater, and D. Vaněk, J. Math. Phys. **42**, 4050 (2001).
[24] M. Frigerio and M. G. A. Paris, "Swift chiral quantum walks," arXiv:2207.05168 (2022).
[25] L. Novo and S. Ribeiro, Phys. Rev. A **103**, 042219 (2021).
[26] M. Pant, H. Krovi, D. Towsley, L. Tassiulas, L. Jiang, P. Basu, D. Englund, and S. Guha, npj Quantum Inf. **5**, 25 (2019).
[27] J. Chung, E. M. Eastman, G. S. Kanter, K. Kapoor, N. Lauk, C. H. Peña, R. K. Plunkett, N. Sinclair, J. M. Thomas *et al.*, IEEE Trans. Quantum Eng. **3**, 22361190 (2022).
[28] L. Banchi, G. Coutinho, C. Godsil, and S. Severini, J. Math. Phys. **58**, 032202 (2017).
[29] M. G. A. Paris, C. Benedetti, and S. Olivares, Symmetry **13**, 96 (2021).
[30] S. L. Braunstein and C. M. Caves, Phys. Rev. Lett. **72**, 3439 (1994).
[31] M. G. A. Paris, Int. J. Quantum Inf. **7**, 125 (2009).
[32] G. Brida, I. P. Degiovanni, A. Florio, M. Genovese, P. Giorda, A. Meda, M. G. A. Paris, and A. Shurupov, Phys. Rev. Lett. **104**, 100501 (2010).
[33] C. Benedetti, F. Buscemi, P. Bordone, and M. G. A. Paris, Phys. Rev. A **89**, 032114 (2014).
[34] M. A. C. Rossi and M. G. A. Paris, Phys. Rev. A **92**, 010302 (2015).
[35] C. Benedetti and M. G. A. Paris, Phys. Lett. A **378**, 2495–2500 (2014).
[36] C. Benedetti, F. Salari Sehdaran, M. H. Zandi, and M. G. A. Paris, Phys. Rev. A **97**, 012126 (2018).
[37] F. Chapeau-Blondeau, Phys. Lett. A **447**, 128300 (2022).
[38] J. Liu, X.-X. Jing, and X. Wang, Sci. Rep. **5**, 8565 (2015).
[39] A. De Pasquale, D. Rossini, P. Facchi, and V. Giovannetti, Phys. Rev. A **88**, 052117 (2013).
[40] A. Candeloro, S. Razavian, M. Piccolini, B. Teklu, S. Olivares, and M. G. A. Paris, Entropy **23**, 1353 (2021).